This is an Accepted Manuscript of an article published by Springer Nature in Journal of Physiology and Biochemistry, 68 (2), 205 - 218 on June 2012, available at: https://doi.org/10.1007/s13105-011-0132-0

Lack of reelin modifies the gene expression in the small intestine of mice

P. García-Miranda , M. D. Vázquez-Carretero G. Gutiérrez, M. J. Peral, A. A. Ilundáin

Departamento de Fisiología y Zoología, Facultad de Farmacia, Universidad de Sevilla, c/o Profesor García González, no. 2, 41012 Sevilla, Spain

Abstract We recently demonstrated that the mucosa of the small intestine of the rat expresses reelin and some components of its signaling system. The current study evaluates whether reelin affects the intestinal gene expression profile using microarray analysis and reeler mice, a natural mutant in which reelin is not expressed. The effect of the mutation on body weight and intestinal morphology is also evaluated. The mutation reduces body and intestinal weight during the first 2 months of age and modifies the morphology of the crypts and villi. For the microarray assays, total RNA was obtained from either isolated epithelial cells or intact small intestine. Of the 45,101 genes present in the microarray the mutation significantly alters the expression of 62 genes in the isolated epithelial cell samples and of 84 in the intact small intestine. The expression of 83% of the genes tested for validation was substantiated by reverse transcriptase polymerase chain reaction. The mutation notably up-regulates genes involved in intestinal metabolism, while it down-regulates genes related with immune response, inflammation, and tumor development. Genes involved in cell proliferation, differentiation, apoptosis, membrane transport and cytoskeleton are also differently expressed in the reeler mice as compared with the control. This is the first report showing that the lack of reelin modifies intestinal

morphology and gene expression profile and suggests a role for reelin in intestinal epithelium homeostasis.

Keywords Genomic · Reelin · Intestine · Epithelium · Isolated epithelial cells · Immune response

Introduction

The epithelium of the small intestine consists of a highly dynamic cell population that undergoes a rapid turnover throughout life in conjunction with structural and functional differentiation. Two compartments of cells are distinguished in the adult mammalian epithelium: the proliferating cells in the crypts and the nonproliferating, differentiated cells in the villi. Proliferation stops at the crypt–villus junction and the new cells either move downward and settle at the base of the crypts as differentiated Paneth cells or migrate upward along the villus while differentiating into enterocytes, enteroendocrine and mucus-secreting goblet cells. When the cells reach the villus tip, they eventually undergo apoptosis and are extruded into the gut lumen [32, 38]. Cell proliferation, migration, differentiation and apoptosis are spatially and temporally regulated, but the molecular mechanisms and the genes critical for epithelial cell positioning are still uncertain and undefined.

Reciprocal interactions between intestinal epithelial cells and the extracellular matrix regulate cell proliferation, migration, differentiation and entry into a death program [40]. Within the extracellular matrix, the myofibroblasts located beneath the epithelia play a key role in the homeostasis of the crypt–villus unit. They secret an extensive repertoire of agents as well as express receptors for many of these ligands, allowing information flow in both directions: to and from the intestinal epithelium and the lamina propria [33]. We recently reported [13] that rat intestinal mucosa expresses reelin and some components of its signaling system, such as its receptors VldlR and ApoER2 and its effector protein Dab1 (disabled1). Although crypt cells, epithelial cells and myofibroblasts express ApoER2, VldlR and Dab1 genes, reelin expression was restricted to myofibroblats. Based on this pattern of expression, we suggested that the reelin released by the myofibroblats to the extracellular matrix might act on the crypts and epithelial cells and regulate the dynamics of the crypt–villus units [13].

Since the report of García-Miranda et al. [13] is the only report on intestinal reelin expression, nothing is known on the role of reelin in such tissue so far. To better understand and elucidate the role of reelin in intestinal mucosa homeostasis, we examined the intestinal gene expression of control and reeler mice using the gene microarray technique, which allows the simultaneous transcriptional expression of thousands of host genes. The reeler mouse is a natural mutant in which reelin is absent [7]. A preliminary report of some of these results was published as an abstract

[30].

Materials and methods

Chemicals

Unless otherwise indicated, the reagents used in this study were from Sigma-Aldrich, Madrid, Spain.

Animals and genotype study

Reeler (rl) is a spontaneous autosomal recessive mutation [7]. Heterozygous (rl^+/rl^-) mice C57BL/6 were purchased from Jackson Laboratories (Bar Harbor, ME). Control (rl^+/rl^+, wild type) and homozygous mutant reeler (rl^-/rl^-) mice were obtained by heterozygous crossings. Suckling (15 days postpartum), weaning (21 days postpartum) and adult (1, 2, 3 and 18 months old) mice were used. The animals were housed in a 12:12-h light–dark cycle and fed ad libitum with Global 2019 extruded rodent diet (Harlan Ibérica S.L.) with free access to tap water. The mice were genotyped by polymerase chain reaction (PCR) analysis of genomic DNA, as described by D'Arcangelo et al. [8].

The mice were killed by cervical dislocation. They were humanely handled and killed in accordance with the European Council legislation 86/609/EEC concerning the protection of experimental animals.

Morphological studies

The small intestine was rapidly removed from the mice, washed with ice-cold saline solution and fixed by incubation with phosphate-buffered saline (PBS) containing 4% paraformaldehyde at 4°C overnight. Cryosections (10 μm) were stained with hematoxylin and eosin procedure.

Measurements of villus (height, width and number) and crypts (diameter and depth) parameters were done on at least 10 well-oriented full-length crypt–villus units per animal. Morphometry was performed by Spot Advance 3.5.4.1. Program analysis of digitally acquired images (Diagnostic Instrument, Inc.).

Isolation of intestinal epithelial cells

Epithelial cells were isolated from the small intestine of the control and reeler mice as previously described [13]. Briefly, the small intestine was rapidly removed and washed with ice-cold saline solution. Intestinal segments (1 cm) were incubated at room temperature in PBS buffer containing 1 mM dithiothreitol for 15 min, followed by a 30-min incubation period at 37°C in a calcium- and magnesium-free PBS buffer containing 1 mM EDTA and 2 mM glucose. Following the incubation, the tissues were vortexed for 30 s, the loosened epithelial cells were filtered through a 60-μm nylon textile and collected by centrifugation and resuspension in PBS.

Microarray analysis

The total RNA samples were submitted to the Instituto de Investigación del Cáncer (Universidad de Salamanca-CSIC (Consejo Superior de Investigaciones Científicas), Salamanca, Spain). The samples were processed according to Affymetrix protocols. Affymetrix Genechip Mouse Genome 430 2.0 arrays were used. The expression of 45,101 genes is analyzed in each microarray.

Total RNA was extracted from either the isolated epithelial cells of the control (four replicates) and reeler (four replicates) mice or the intact total small intestine (duodenum, jejunum and ileum) of the control (three replicates) and reeler (three replicates) mice of 1 month old, as described by García-Miranda et al. [13].

Fluorescence intensity values generated from hybridized and labeled genechips were analyzed using DChip [23]. DChip was also used to normalize the data with the Invariant Set method and the model-based expression values were calculated with the PM-only option. Differentially expressed genes were statistically filtered using a Student *t*-test, FDR (false discovery rate)-adjusted p value ≤ 0.01 and an estimated fold- change relative to control values ≥ 1.5. Assignments of filtered genes into functional categories were per- formed by using FatiGO server (http://fatigo.bioinfo. cnio.es). A more refined search of the functions of the genes was obtained by searching in the PubMed.

Real-time PCR analysis

Reverse transcriptase PCR (RT-PCR) was performed as previously

described by García-Delgado et al. [12]. Analysis confirmed a single PCR product at the predicted melting temperature. Primers for the genes tested are given in Table 1. β-Actin and glyceraldehyde-3-phosphate dehydrogenase (GAPDH) were used as reference genes for samples normalization. Analyses of real-time PCR were done using the comparative Ct method with the Gene Expression Macro software supplied by BioRad.

Statistical analysis

Data are presented as mean ± SEM for *n* separated animals. In the figures, the vertical bars that represent the SEM are absent when they are less than a symbol height. One-way analysis of variance (ANOVA) followed by Newman–Keuls' test was used for multiple comparisons (GraphPad Prism Program). Differences were set to be significant for $p < 0.05$.

Results

Body and small intestine weights

Figure 1 shows that the body and small intestinal weights of the reeler mice are similar to those of the wild-type littermates during the suckling period.

During the weaning period, the body and intestinal weight gains are slower in the reeler than the wild- type mice. The reeler mice show a spurt in growth during adulthood and at 1.5 years old (18 months old) their body and intestinal weights are similar to those of the wild-type mice.

Intestinal morphology

Table 2 summarizes the measurements of intestinal morphological parameters made in wild-type and reeler mice of different ages.

In both types of mice, the number, length and width of the villi, as well as the depth, diameter and number of the crypts significantly increase during the weaning period. Thereafter, the morphology and number of the villi and crypts remain fairly invariant. The mutation significantly decreases the width of villi and increases their number during the first 2 months of life. From 1 to 2 months of age, the depth and diameter of the crypts are slightly reduced by the mutation. The rest of the parameters measured and

listed in Table 2 are not significantly modified by the mutation.

Intestinal gene expression in control and reeler mice

The gene expression profiles of isolated epithelial cells and of intact small intestine of control and reeler mice were analyzed by microarray hybridization assays. Isolated epithelial cells were used to distin- guish epithelial gene expression profile from that of the whole small intestine. Crypt cells could not be used as a source of RNA because of the large number of mice required to obtain the amount of total RNA needed for the microarray studies.

The fluorescence intensity values generated from the isolated epithelial cells and those from the intact intestine samples were normalized separately. To focus on only differentially expressed genes, the 45,101 genes present on each array were filtered on a fold-change $\geq$ 1.5-fold relative to control and a $p \leq 0.01$ for *t*-test. This filtering yields a list of 62 differently expressed genes in the isolated epithelial cells samples and of 84 in the intact small intestine. This represents less than a 0.2% gene expression profile modification. In the isolated epithelial cells, 31 genes are up-regulated and 31 are down-regulated. In the intact small intestine, the up-regulated and down-regulated genes are 23 and 61, respectively. The fluorescence values also reveal that reelin expression is detected in the intact intestine of the control mice, but it is absent from both the intact intestine of the reeler mice and the isolated epithelial cells of either type of mice.

Grouping the genes according to their biological functions

The lists of differentially expressed genes were analyzed using the FatiGO bioinformatics tool to assign the genes to functional categories. A more refined search of the functions of the genes was obtained by PubMed searches. The results are given in Tables 3 and 4 and Fig. 2. The classification of genes to specific cellular function is difficult because many genes participate in more than one biological function. For simplicity, we have listed the genes in one single functional category. The miscellaneous group contains those genes with either an unknown function or a described function difficult to ascribe to any particular functional group

The most overrepresented ontological category of down-regulated genes

and with the biggest fold-change values, both in the intact intestine and in the isolated epithelial cells, is associated with the intestinal defence, while the most overrepresented up-regulated genes are associated with metabolism and membrane transport. Other genes differentially expressed in the reeler mice are associated with proliferation, cytoskeleton, circadian rhythms, development, differentiation and apoptosis. Verification of microarray analysis by real-time PCR analysis

To confirm the microarray results, 12 genes from different functional groups were selected for validation by real-time PCR. Four genes were chosen from the list of differentially expressed genes found in the intact intestine and 8 from those of the isolated epithelial cells list. We selected genes described as regulators of intestinal epithelium homeostasis. The RT-PCR was performed on total RNA obtained from either isolated epithelial cells or the intact small intestine of the control and reeler mice. The PCR and the microarray ratios are given in Fig. 3. Of the 12 genes selected, 10 demonstrate similar trends of change by both microarray and real-time PCR analysis; 1 gene shows opposite changes with microarray and real-time PCR analysis, and 1 gene shows up-regulation of expression with microarray analysis and nondifferent expression with real-time PCR. Thus, approximately 83% of the genes tested are validated.

Discussion

We recently reported for the first time that the rat intestinal mucosa expresses reelin and that this expression was restricted to the myofibroblasts located beneath the crypt and intestinal epithelia cells. We suggested that the reelin released to the extracellular matrix may be involved in the homeostasis of the crypt–villus unit [13]. The current data corroborate our previous observations in that the isolated epithelial cells of the control mice do not express reelin and demonstrate for the first time that reelin may play a role in intestinal homeostasis because its absence modifies the gene expression profile of the mice intestine.

Reelin-related changes in the amount of gene transcripts were found in less than 0.2% genes of the 45,000 genes tested. This indicates that the intestinal response to the absence of reelin is not generalized, but rather narrow. It also suggests that the observed changes in the gene expression profile may reflect the alteration of biological functions, even though the absence of reelin did not produce gross morphological changes. However,

only approximately 37% of the modified genes were known to function in the intestine and the intestinal function of the 63% additional genes has been inferred from those previously described in other cell types.

Reciprocal interactions between the epithelial cells and the extracellular matrix components control crypt–villus unit homeostasis and hence, the gene expression changes observed in the isolated epithelial cells could result directly from the lack of reelin and/or be secondary to changes induced by the lack of reelin on other mucosal cells. This is why the observations made in intact intestine and those made in isolated epithelial cells are discussed together. In theory, the genes differentially expressed in the isolated epithelial cells should also be differentially expressed in the intact intestine microarrays. However, only three differentially expressed genes appear simultaneously in both types of samples. One reason for this may be that the epithelial cells represent a relative small pool in the total intestine, so that in the total RNA obtained from the intact intestine the amount of RNA belonging to the cells lining the villi is relatively small. In addition, the epithelium contains different cell types that differentiate as they migrate upward along the villus and hence, their gene expression profile varies [25].

From weaning to about 2 months of age the body weight of the reeler mice is lower than that of the control mice, which agrees with the observations of Lombardero et al. [24]. This could result from changes in the total absorptive surface area. However, the observed increase in the number of villi could be compensated by the decrease in their width, so that the total absorptive surface area would not change. The lower body weight of the reeler mice could also be due to retardation in the intestinal adaptation to dietary transition and/or from the ataxia developed by the reeler mice [11], which will impair feeding and, hence, will lead to caloric restriction. The following observations support the latter point of view. The mutation alters the expression of a significant number of genes involved in cell metabolism and lipid transport, such as Ppara and Abca1 genes, which appear differentially expressed in the isolated cells microarray assay, and Ppara, Angptl4, CD36, Ucp2, Scarb2 and Ostb genes, which were detected in the intact intestine assays. The expression of Ppara, Angptl4 and Ucp2 genes is up-regulated in the reeler mice. Ppara and Angptl4 genes are activated by fasting or caloric restriction and trigger metabolic adaptations to minimize the use of protein and carbohydrates as fuel [20, 21]. The uncoupling protein UCP2 decreases the oxidation of glucose, while it favors the oxidation of fatty acids (see Ref. [10], for a review]. The other genes mentioned above code for proteins involved in the intestinal transport of lipids. The expression of CD36, Abca1 and Scarb2 is up-regulated and that of Ostb is down-regulated. The CD36 product mediates fatty acid

uptake by the enterocytes apical membrane [9]; that of Abca1 transports cholesterol and phospholipids [2], that of Ostb transports bile acids across the basolateral membrane of enterocytes [3], and that of Scarb2 is a membrane receptor that, after binding to the high-density lipoprotein, produces mobilization of stored cholesterol esters and efflux of cellular-free cholesterol [29]. Therefore, the changes in gene expression induced by the mutation favor lipid metabolism, a situation expected to occur under fasting or caloric restriction. All these observations suggest that reelin may be involved in the adaptive response to nutritional stress.

The mutation also affects the expression of genes described as components of signaling pathways that regulate proliferation, migration, differentiation and apoptosis of intestinal epithelial cells. It down-regulates the expression of the Cdx2, Arrb1 and Pycard genes and up-regulates that of the EphA1, Pik3ca and Bmp1 genes. Except for the Bmp1 gene, detected in the intact intestine assays, the other genes were detected in the isolated cells assays. The transcription factor Cdx2 [17, 18], the product of Arrb1, β1-arrestin [5] and that of Pik3ca, the α- catalytic subunit of phosphatidylinositol 3-kinase [22, 37] regulate intestinal epithelial cell differentia- tion and proliferation. The product of EphA, ephrin A, coordinates the migration and proliferation of the intestinal stem cells [6]. The product of Bmp1 regulates the deposition of fibrous extracellular matrix [36] and stimulates the BMP signaling pathway [15], a pathway described as a negative regulator of intestinal cell proliferation [19]. Pycard is a proapoptotic gene [28] that is expressed by the intestinal epithelial cells [27]. All these findings suggest a role for reelin in the dynamics of the crypt–villus unit and agree with the observations made in the brain showing that (1) the lack of reelin reduces proliferation, differentiation and migration of stem cells [26] and (2) reelin modifies the activity of the PIK3 [4].

Interestingly, the largest number of differentially expressed genes in both isolated cells and intact intestine microarray assay are the genes related with intestinal immune response, inflammation and tumor development. Only the genes with reported intestinal function will be discussed and those chosen were detected in the intact intestine assays. Alterations in the immune system of the reeler mice were reported by Green-Johnson et al. [16]. They found a defective function in T-cell and macrophage populations. The current results reveal that the reeler mutation down-regulates genes coding for chemokines (i.e., Cxcl10 and Ccl3 genes), for interferon-induced proteins and for proteins involved in antiviral innate immune response such as Duoxa2 [14], Isg15, Herc5 and Usp18. The

last three genes belong to the “Isg15-conjugation pathway” [31]. The expression of genes involved in intestinal inflammatory response, tumor development and tissue injury is also significantly modified by the mutation. It down-regulates the expression of the Dmbt1 and Pycard genes, and it has been reported that (1) Dmbt1 deletion increased the intestinal susceptibility to inflammation [35] and (2) Pycard protects the intestine against colitis-associated cancer develop- ment [1]. On the other hand, the mutation up-regulates the expression of FoxM1 and Tm4sf4. The former has been associated with carcinogenesis [39] and Tm4sf4 accelerates tissue injury [34]. All these observations suggest that reelin might increase the resistance of the intestine to the development of infectious and noninfectious pathologies and led us to investigate whether intestinal reelin expression is modified under pathological conditions. Preliminary observations reveal that reelin expression is decreased in human colon tumors (unpublished observations) and support the suggested hypothesis.

In conclusion, this is the first study that examines the effect of reelin on the gene expression profile of the mice small intestine. The findings suggest that reelin may regulate intestinal homeostasis. Further understanding of the intestinal functions of reelin may have the potential to reveal the basic mechanisms underlying the intestinal epithelium homeostasis and its response to pathologies.

Acknowledgements This work was supported by a grant from the Junta de Andalucía (CTS 5884) and by a fellowship from the Spanish Ministerio de Educación y Ciencia (AP2007-04201) to M.D. Vázquez-Carretero. We thank Dr. E. Soriano from the University of Barcelona for supplying the reeler mice used at the beginning of this study and Dr. O. Pintado from the University of Sevilla for his technical advice

References

1. Allen IC, TeKippe EM, Woodford RM, Uronis JM, Holl EK, Rogers AB, Herfarth HH, Jobin C, Ting JP (2010) The NLRP3 inflammasome functions as a negative regulator of tumorigenesis during colitis-associated cancer. J Exp Med 207:1045–1056
2. Attie AD (2007) ABCA1: at the nexus of cholesterol, HDL and atherosclerosis. Trends Biochem Sci 32:172–179
3. Ballatori N, Fang F, Christian WV, Li N, Hammond CL (2008) Ostalpha–Ostbeta is required for bile acid and conjugated steroid disposition in the intestine, kidney, and liver. Am J Physiol Gastrointest Liver Physiol 295:179–186
4. Beffert U, Morfini G, Bock HH, Reyna H, Brady ST, Herz J (2002) Reelin-mediated signalling locally regulates protein kinase B/Akt and glycogen synthase kinase 3beta. J Biol Chem 277:49958–49964
5. Bryja V, Gradl D, Schambony A, Arenas E, Schulte G (2007) Beta-arrestin is a necessary component of Wnt/beta-catenin signaling in vitro and in vivo. Proc Natl Acad Sci USA 104:6690–6695
6. Crosnier C, Stamataki D, Lewis J (2006) Organizing cell renewal in the intestine: stem cells, signals and combi- natorial control. Nat Rev Genet 7:349–359
7. D'Arcangelo G, Miao GG, Chen SC, Soares HD, Morgan JI, Curran T (1995) A protein related to extracellular matrix proteins deleted in the mouse mutant reeler. Nature 374:719–723
8. D'Arcangelo G, Miao GG, Curran T (1996) Detection of the reelin breakpoint in reeler mice. Brain Res Mol Brain Res 39:234–236
9. Drover VA, Nguyen DV, Bastie CC, Darlington YF, Abumrad NA, Pessin JE, London E, Sahoo D, Phillips MC (2008) CD36 mediates both cellular uptake of very long chain fatty acids and their intestinal absorption in mice. J Biol Chem 283:13108–13115
10. Emre Y, Nübel T (2010) Uncoupling protein UCP2: when mitochondrial activity meets immunity. FEBS Lett 584:1437–1442
11. Falconer DS (1951) Two new mutants "trembler" and "reeler" with neurological actions in the house mouse. J Gent 50:192–205
12. García-Delgado M, García-Miranda P, Peral MJ, Calonge ML, Ilundáin AA (2007) Ontogeny up-regulates renal Na (+)/Cl(−)/creatine transporter in rat. Biochim Biophys Acta 1768:2841–2848
13. García-Miranda P, Peral MJ, Ilundáin AA (2010) Rat small intestine expresses the reelin-Dab1 signalling pathway. Exp Physiol 223:451–459
14. Gattas MV, Forteza R, Fragoso MA, Fregien N, Salas P, Salathe M, Conner GE (2009) Oxidative epithelial host defense is regulated by infectious and inflammatory stimuli. Free Radic Biol Med 47:1450–1458
15. Ge G, Greenspan DS (2006) Developmental roles of the BMP1/TLD metalloproteinases. Birth Defects Res C Embryo Today 78:47–68
16. Green-Johnson JM, Zalcman S, Vriend CY, Nance DM, Greenberg AH (1995) Suppressed T cell and macrophage function in the "reeler" (rl/rl) mutant, a murine strain with elevated cerebellar norepinephrine concentration. Brain Behav Immun 9:47–60

17. Guo RJ, Funakoshi S, Lee HH, Kong J, Lynch JP (2010) The intestine-specific transcription factor Cdx2 inhibits beta-catenin/TCF transcriptional activity by disrupting the beta-catenin–TCF protein complex. Carcinogenesis 31:159–166
18. Guo RJ, Suh ER, Lynch JP (2004) The role of Cdx proteins in intestinal development and cancer. Cancer Biol Ther 3:593–601
19. He XC, Zhang J, Tong WG, Tawfik O, Ross J, Scoville DH, Tian Q, Zeng X, He X, Wiedemann LM, Mishina Y, Li L (2004) BMP signalling inhibits intestinal stem cell self-renewal through suppression of Wnt–beta-catenin signalling. Nat Genet 36:1117–1121
20. Kersten S, Lichtenstein L, Steenbergen E, Mudde K, Hendriks HF, Hesselink MK, Schrauwen P, Müller M (2009) Caloric restriction and exercise increase plasma ANGPTL4 levels in humans via elevated free fatty acids. Arterioscler Thromb Vasc Biol 29:969–974
21. Kersten S, Seydoux J, Peters JM, Gonzalez FJ, Desvergne B, Wahli W (1999) Peroxisome proliferator-activated receptor alpha mediates the adaptive response to fasting. J Clin Invest 103:1489–1498
22. Laprise P, Chailler P, Houde M, Beaulieu JF, Boucher MJ, Rivard N (2002) Phosphatidylinositol 3-kinase controls human intestinal epithelial cell differentiation by promoting adherens junction assembly and p38 MAPK activation. J Biol Chem 277:8226–8234
23. Li C, Hung Wong W (2001) Model-based analysis of oligonucleotide arrays: model validation, design issues and standard error application. Genome Biol 2 RESEARCH0032
24. Lombardero M, Kovacs K, Horvath E, Salazar I (2007) Hormonal and morphological study of the pituitaries in reeler mice. Int J Exp Pathol 88:165–173
25. Mariadason JM, Nicholas C, L'Italien KE, Zhuang M, Smartt HJ, Heerdt BG, Yang W, Corner GA, Wilson AJ, Klampfer L, Arango D, Augenlicht LH (2005) Gene expression profiling of intestinal epithelial cell maturation along the crypt–villus axis. Gastroenterology 128:1081– 1108
26. Massalini S, Pellegatta S, Pisati F, Finocchiaro G, Farace MG, Ciafrè SA (2009) Reelin affects chain-migration and differentiation of neural precursor cells. Mol Cell Neurosci 42:341–349
27. Masumoto J, Taniguchi S, Nakayama J, Shiohara M, Hidaka E, Katsuyama T, Murase S, Sagara J (2001) Expression of apoptosis-associated speck-like protein containing a caspase recruitment domain, a pyrin N-terminal homology domain-containing protein, in normal human tissues. J Histochem Cytochem 49:1269–1275
28. McConnell BB, Vertino PM (2004) TMS1/ASC: the cancer connection. Apoptosis 9:5–18
29. Mulcahy JV, Riddell DR, Owen JS (2004) Human scavenger receptor class B type II (SR-BII) and cellular cholesterol efflux. Biochem J 377:741–747
30. Peral MJ, García-Miranda P, Vázquez-Carretero MD, Gutiérrez G, Ilundain AA (2009) Gene expression profile of the small intestine in reeler mice. J Physiol Sci 59:529, Abstract
31. Pitha-Rowe IF, Pitha PM (2007) Viral defense, carcinogenesis and ISG15: novel roles for an old ISG. Cytokine Growth Factor Rev 18:409–417
32. Potten CS (1992) The significance of spontaneous and induced apoptosis in the gastrointestinal tract of mice. Cancer Metastasis Rev 1:179–195
33. Powell DW, Mifflin RC, Valentich JD, Crowe SE, Saada JI, West AB (1999)

Myofibroblasts. I. Paracrine cells impor- tant in health and disease. Am J Physiol 277:1–9
34. Qiu J, Liu Z, Da L, Li Y, Xuan H, Lin Q, Li F, Wang Y, Li Z, Zhao M (2007) Overexpression of the gene for transmembrane 4 superfamily member 4 accelerates liver damage in rats treated with CCl4. J Hepatol 46:266–275
35. Renner M, Bergmann G, Krebs I, End C, Lyer S, Hilberg F, Helmke B, Gassler N, Autschbach F, Bikker F, Strobel- Freidekind O, Gronert-Sum S, Benner A, Blaich S, Wittig R, Hudler M, Ligtenberg AJ, Madsen J, Holmskov U, Annese V, Latiano A, Schirmacher P, Amerongen AV, D'Amato M, Kioschis P, Hafner M, Poustka A, Mollenhauer J (2007) DMBT1 confers mucosal protection in vivo and a deletion variant is associated with Crohn's disease. Gastroenterology 133:1499–1509
36. Scott IC, Imamura Y, Pappano WN, Troedel JM, Recklies AD, Roughley PJ, Greenspan DS (2000) Bone morphogenetic protein-1 processes probiglycan. J Biol Chem 275:30504–30511
37. Sheng H, Shao J, Townsend CM Jr, Evers BM (2003) Phosphatidylinositol 3-kinase mediates proliferative signals in intestinal epithelial cells. Gut 52:1472–1478
38. Van der Flier LG, Clevers H (2009) Stem cells, self-renewal, and differentiation in the intestinal epithelium. Annu Rev Physiol 7:241–260
39. Wang Z, Ahmad A, Li Y, Banerjee S, Kong D, Sarkar FH (2010) Forkhead box M1 transcription factor: a novel target for cancer therapy. Cancer Treat Rev 36:151–156
40. Yeaman C, Grindstaff KK, Nelson WJ (1999) New perspectives on mechanisms involved in generating epithelial cell polarity. Physiol Rev 79:73–98

Gene	GenBank ID	Sense (5′-3′)	Antisense (5′-3′)
Bmp1	NM_009755	agttctcagacagcaaacag	ccaatcacaaacgggatgac
Clca2	NM_030601	aaaagtgcgtgtccaggcaa	ctccagaggttactctgttga
Dmbt1	NM_007769	gaaatgccaggtttggacag	tcagttggatagaacacatcgt
Dtx3l	NM_001013371	tccataacaaacctgtgacca	acagagttagaaacgagccc
Arrb1	NM_177231	gagtctacgtgacactgacc	gggatctcaaagtgtaaggg
Ppara	NM_011144	catcgagtgtcgaatatgtg	tcagatcttggcattcttcc
Cdx2	NM_007673	aactacaggagccagaggca	agggacaggaagtccaggtt
Frk	NM_010237	gtcagtagtaattgagaatccagg	cgtaattggaaggaatgtacc
Pycard	NM_023258	gagtacagccagaccaggac	aggatggaacaaagctgaagag
Pik3ca	NM_008839	gtgactttagaatgcctccgt	ttcttcacggttgcctactg
Ap2b1F	NM_001035854	gggtggacaagattacagag	agtaagttgcgtttgggtg
Epha1	NM_023580	caacaaatgctaaacgggacac	gaaggtctctttgcatccca
β-Actin	NM_007393.2	acccacactgtgcccatcta	cggaaccgctcattgcc
GAPDH	NM_008084.2	caccagggctgccatttg	ctggaacatgtagagcatgt

Table 1 Oligonucleotides sequences used for real-time PCR assays. Oligonucleotides were chosen according to the cDNA sequences entered in GenBank and designed using PerlPrimer Program v1.1.14

Table 2. Morphometric parameters of small intestinal mucosa in reeler and control mice

	Villi						Crypts				
	Length		Width		Number per section		Depth		Diameter		Number p
Age (days)	C	R	C	R	C	R	C	R	C	R	C
15	329±7.0	308±7.0	52.4±1.3	49.8±1.0	45.7±0.6	47.9*±0.6	45.5±1.3	45.1±0.9	29.6±0.6	28.9±0.6	80.6±2
30	468^{+}±8.0	480^{+}±9.0	72.8^{+}±1.3	66.4**$^{,+}$±1.3	45.4±1.6	51.7**$^{,++}$±0.8	81.4^{+}±1.4	71.4**$^{,+}$±2.2	50.5^{+}±2.2	46.4^{+}±1.8	102.6^{+}±5.9
60	557^{+}±7.0	530^{+}±11	89.9^{+}±2.5	67.1**$^{,+}$±1.4	39.7^{+}±0.5	45.1**$^{,++}$±0.6	92.5^{+}±1.8	80.4**$^{,+}$±1.4	46.1^{+}±1.4	41.2*$^{,+}$±1.1	124.9^{+}±2.4
550	432^{+}±7.0	507^{+}±13	85.0^{+}±2.0	84.4^{+}±2.3	42.5^{++}±2.3	50.6*$^{,++}$±1.2	93.5^{+}±1.7	91.4^{+}±2.0	45.9^{+}±1.3	42.4^{+}±1.3	141.7^{+}±4.4

The morphology of small intestinal mucosa from reeler and control mice are compared. Measurements are shown in micrometers except for the number of villi and crypts. Five reeler (R) and five control (C) mice per age were used. One-way ANOVA showed the effect of the age and of the mutation on intestinal morphology (p<0.001). Newman–Keuls´ test: *p<0.001 and **p<0.05 as compared with reeler versus wild-type mice; $^{+}$ p<0.001 and $^{++}$ p <0.05 as compared with 15- day-old mice

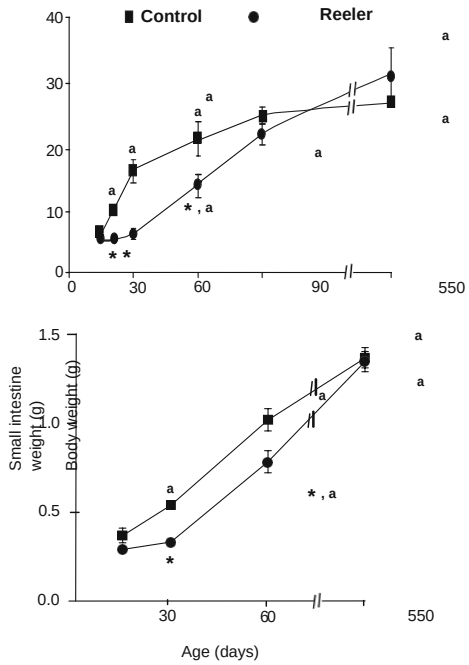

Fig. 1 Body and small intestinal weights of the control and reeler mice versus age. Data are presented as the mean ± SE of five different animals per age. One-way ANOVA showed an effect of the age and mutation on body and small intestine weights (p<0.001). Newman–Keuls´ test, *p<0.001 as com- pared with reeler versus wild type-mice and ^{a}p <0.01 as compared with 15-day-old mice

Table 3 List of the differentially modified transcripts identified by microarray analysis in the isolated epithelial cells of reeler mice

Gene symbol	Accession number	Gene name	Fold-change	*p*
Apoptosis				
Pycard	BG084230	PYD and CARD domain containing	−1.72	0.007
Ing3	BB020556	Inhibitor of growth family, member 3	2.66	0.001
Circadian rhythm				
Arntl	BC011080	Aryl hydrocarbon receptor nuclear translocator-like	−2.17	0.003
Npas2	BG070037	Neuronal PAS domain protein 2	−2.07	0.002
Cytoskeleton				
St5	AK008100	Suppression of tumorigenicity 5	−1.87	0.001
Arrb1	AK004614	Arrestin, beta 1	−1.82	0.001
Mical1	NM_138315	Microtubule-associated monooxygenase, calponin and LIM domain containing 1	−1.58	0.005
Fus	AF224264	Fusion, derived from malignant liposarcoma	1.94	0.009
Ric3	BB312654	Resistance to inhibitors of cholinesterase 3 homolog	2.05	0.008
Defence and immune systems				
Nfil3	AY061760	Nuclear factor, interleukin 3, regulated/similar to NFIL3/E4BP4 transcription factor	−2.99	0.001
Aldh18a1	NM_019698	Aldehyde dehydrogenase 18 family, member A1	−1.80	0.004
Pdia4	J05186	Protein disulfide isomerase associated 4	−1.73	0.003
Ccnjl	BM120177	Cyclin J-like	−1.71	0.002
Sdf2l1	NM_022324	Stromal cell-derived factor 2-like 1	−1.69	0.004
Irf2bp2	BB183385	Interferon regulatory factor 2 binding protein 2	−1.67	0.003
Rrbp1	AK019964	Ribosome-binding protein 1	−1.63	0.001
Batf2	AK016990	Basic leucine zipper transcription factor, ATF-like 2	−1.60	0.006
Endod1	BF168366	Endonuclease domain containing 1	−1.59	0.002
Ttc7	BB235116	Tetratricopeptide repeat domain 7	−1.58	0.010
Mpst	NM_138670	Mercaptopyruvate sulfurtransferase	−1.57	0.008
Cd8b1	BF682469	CD8 antigen, beta-chain 1	−1.56	0.008
Irf8	BG069095	Interferon regulatory factor 8	−1.55	0.004
Sema6d	BB462688	Sema domain, transmembrane domain and cytoplasmic domain (semaphorin) 6D	−1.55	0.004
Muc13	NM_010739	Mucin 13, epithelial transmembrane	−1.54	0.007
Nub1	NM_016736	Negative regulator of ubiquitin-like proteins 1	−1.53	0.009
Hsp90ab1	BI154147	Heat shock protein 90 kDa alpha class B, member 1	−1.51	0.005
Clec4d	NM_010819	C-type lectin domain family 4, member d	1.51	0.005
Sod1	AV261043	Superoxide dismutase 1, soluble	1.58	0.007
Herpud1	AI835088	Homocysteine-inducible, endoplasmic reticulum stress-inducible, ubiquitin-like domain member 1	1.70	0.004
Cat	NM_009804	Catalase	1.88	0.009
Development and differentiation				
E2f2	BB543028	E2F transcription factor 2	−1.65	0.009
Cdx2	NM_007673	Caudal-type homeo box 2	−1.55	0.007
Mall	AV378589	Mal, T-cell differentiation protein-like	−1.54	0.003
Gmfb	BG228815	Glia maturation factor, beta	1.56	0.004
Csrp1	BF124540	Cysteine and glycine-rich protein 1	1.64	0.001
Frk	NM_010237	Fyn-related kinase	1.69	0.003

Table 3 (continued)

Gene symbol	Accession number	Gene name	Fold-change	*p*
Membrane transport				
Tmem16f	BG074632	Transmembrane protein 16F	1.55	0.009
Tomm7	BB609428	Translocase of outer mitochondrial membrane 7 homolog	1.67	0.002
Vapb	BF303544	Vesicle-associated membrane protein, associated protein B and C	1.74	0.001
Ap2b1	AV271093	Adaptor-related protein complex 2, beta 1 subunit	1.89	0.002
Abca1	BB144704	ATP-binding cassette, subfamily A (ABC1), member 1	2.10	0.006
Metabolism				
Adh1	BC013477	Alcohol dehydrogenase 1 (class I)	1.53	0.001
Cyp3a44	AB039380	Cytochrome P450, family 3, subfamily a, polypeptide 44	1.54	0.004
Acads	NM_007383	Acyl-coenzyme A dehydrogenase, short chain	1.60	0.002
Psap	BM212050	Prosaposin	1.65	0.006
Lipe	NM_010719	Lipase, hormone sensitive	1.75	0.006
Ppara	BC016892	Peroxisome proliferator-activated receptor alpha	1.79	0.008
Akr1c19	BG073853	Aldo-keto reductase family 1, member C19	2.03	0.008
Hsd17b11	NM_053262	Hydroxysteroid (17-beta) dehydrogenase 11	2.95	0.008
Pdk4	NM_013743	Pyruvate dehydrogenase kinase, isoenzyme 4	3.49	0.009
Pck1	AW106963	Phosphoenolpyruvate carboxykinase 1, cytosolic	3.74	0.001
Proliferation				
Pik3ca	BE647269	Phosphatidylinositol 3-kinase, catalytic, alpha polypeptide	1.54	0.008
Igf2r	BG092290	Insulin-like growth factor 2 receptor	1.59	0.001
Epha1	NM_023580	Eph receptor A1	1.91	0.005
Irs2	BE199054	Insulin receptor substrate 2	2.04	0.006
Miscellaneous				
Raly	NM_023130	hnRNP-associated with lethal yellow	−2.11	0.001
Plekha2	NM_031257	Pleckstrin homology domain-containing, family A, member 2	−1.62	0.001
Ankmy2	BC024959	Ankyrin repeat and MYND domain containing 2	−1.59	0.002
Gtf2ir1	AF343349	General transcription factor II I repeat domain-containing 1	−1.56	0.002
Refbp2	NM_019484	THO complex 4/RNA and export factor-binding protein 2	−1.54	0.001
Dnase1	BC014718	Deoxyribonuclease I	1.72	0.003
Myef2	U13262	Myelin basic protein expression factor 2, repressor	1.76	0.005

The transcripts are considered to be modified when they have a fold-change ≥ 1.5 and $p \leq 0.01$. Reeler and control mice are compared. Four reeler and four control mice were used

Table 4 List of the differentially modified transcripts identified by microarray analysis in the small intestine of reeler mice

Gene symbol	Accession number	Gene name	Fold-change	*p*
Apoptosis				
Sh3rf1	BB110728	SH3 domain containing ring finger 1	−1.79	0.008
Defence and immune systems				
Abhd1	NM_021304	Abhydrolase domain containing 1	−8.47	0.002
Duoxa2	NM_025777	Dual oxidase maturation factor 2	−8.21	0.002
Zbp1	AK008179	Z-DNA binding protein 1	−4.41	0.006
Upp1	NM_009477	Uridine phosphorylase 1	−3.37	0.008
Cxcl10	NM_021274	Chemokine (C-X-C motif) ligand 10	−4.00	0.004
Mgat4c	NM_026243	Mannosyl (alpha-1,3-)-glycoprotein beta-1, 4-*N*-acetylglucosaminyltransferase, isozyme C	−3.61	0.006
Herc5	AW208668	Hect domain and RLD 5	−3.57	0.004
Usp18	NM_011909	Ubiquitin-specific peptidase 18	−3.57	0.007
Isg15	AK019325	ISG15 ubiquitin-like modifier	−3.28	0.006
Igtp	NM_018738	Interferon-gamma-induced GTPase	−3.21	0.010
Indo	NM_008324	Indoleamine-pyrrole-2,3-dioxygenase	−3.12	0.006
Trim30	BM240719	Tripartite motif protein 30	−3.11	0.007
Ifit1	NM_008331	Interferon-induced protein with tetratricopeptide repeats 1	−2.83	0.009
Ms4a1	BB236617	Membrane-spanning 4-domains, subfamily A, member 1	−2.75	0.005
Oasl2	BQ033138	2′-5′ oligoadenylate synthetase-like 2	−2.67	0.009
Oas1a	BC018470	2′-5′ oligoadenylate synthetase 1A	−2.66	0.003
Ifi47	NM_008330	Interferon-gamma-inducible protein 47	−2.62	0.004
Klra22	AF419250	Killer cell lectin-like receptor subfamily A, member 22	−2.52	0.003
Irgm	NM_008326	Immunity-related GTPase family, M	−2.20	0.004
Iigp2	NM_019440	Interferon-inducible GTPase 2	−2.12	0.009
Oxct1	AV213379	3-oxoacid CoA transferase 1	−2.11	0.007
Matr3	BI249188	Matrin 3	−2.00	0.005
Hrasls3	BB404920	HRAS-like suppressor 3	−1.99	0.002
Psmb9	NM_013585	Proteasome (prosome, macropain) subunit, beta type 9	−1.97	0.002
Irf7	NM_016850	Interferon regulatory factor 7	−1.96	0.005
Psmb8	NM_010724	Proteasome (prosome, macropain) subunit. beta type 8	−1.88	0.004
Igh-6	AI326478	Immunoglobulin heavy chain 6	−1.87	0.003
Dmbt1	NM_007769	Deleted in malignant brain tumors 1	−1.82	0.009
Dhx58	AF316999	DEXH (Asp-Glu-X-His) box polypeptide 58	−1.75	0.007
Batf2	AK016990	Basic leucine zipper transcription factor, ATF-like 2	−1.73	0.009
Irf8	BG069095	Interferon regulatory factor 8	−1.71	0.003
Epsti1	BF020640	Epithelial stromal interaction 1	−1.63	0.001
Ccl3	NM_011337	Chemokine (C–C motif) ligand 3	−1.61	0.003
Ifit3	NM_010501	Interferon-induced protein with tetratricopeptide repeats 3	−1.60	0.009
Maz	BG243624	MYC-associated zinc finger protein	−1.59	0.009
Pap	NM_011036	Pancreatitis-associated protein (Reg3b)	−1.55	0.005
Tm4sf4	BC010814	Transmembrane 4 superfamily, member 4 (Tetraspanin)	3.65	0.001
Development and differentiation				
Reg3d	AB028625	Regenerating islet-derived 3 delta	−2.39	0.007
Sin3b	AK013202	Transcriptional regulator, SIN3B	−2.16	0.008
Ift172	AK006007	Intraflagellar transport 172 homolog	−1.87	0.005

Table 4 (continued)

Gene symbol	Accession number	Gene name	Fold-change	*p*
Pgr	BB428874	Progesterone receptor	−1.73	0.001
H19	NM_023123	H19 fetal liver mRNA	−1.59	0.006
Bmp1	BG248060	Bone morphogenetic protein 1	1.80	0.006
Homer2	AB017136	Homer homolog 2	1.80	0.008
Membrane transport				
Mfsd4	AI426503	Major facilitator superfamily domain containing 4	−3.60	0.009
Clca2	AV231113	Chloride channel calcium activated 2	−2.14	0.003
Ostb	AV000952	Organic solute transporter beta	−1.76	0.000
Slc19a2	NM_054087	Solute carrier family 19 (thiamine transporter), member 2	1.53	0.002
Ucp2	AW108044	Uncoupling protein 2 (mitochondrial, proton carrier)	1.63	0.001
Abcb1a	M30697	ATP-binding cassette. subfamily B, member 1A	2.12	0.004
Cd36	BB534670	CD36	2.92	0.007
S100g	NM_009789	S100 calcium binding protein G	3.30	0.008
Metabolism				
B3galt5	NM_033149	UDP-Gal:betaGlcNAc beta 1,3-galactosyltransferase. polypeptide 5	−1.94	0.003
Gcnt1	NM_010265	Glucosaminyl (*N*-acetyl) transferase 1, core 2	−1.91	0.009
Gfpt1	AI324119	Glutamine fructose-6-phosphate transaminase 1	−1.66	0.007
Paqr4	BB279185	Progestin and adipoQ receptor family member IV	−1.57	0.004
B3gnt5	BM214359	UDP-GlcNAc:betaGal beta-1,3-*N*-acetylglucosaminyltransferase 5	−1.53	0.008
Pgcp	BB468025	Plasma glutamate carboxypeptidase	−1.52	0.008
Scarb2	BI106458	Scavenger receptor class B, member 2	1.55	0.007
Cyp2d26	NM_029562	Cytochrome P450, family 2, subfamily d, polypeptide 26	1.56	0.004
Dgat2	AK002443	Diacylglycerol *O*-acyltransferase 2	1.64	0.005
Galnt11	BC021504	UDP-*N*-acetyl-alpha- D-galactosamine: polypeptide *N*-acetylgalactosaminyltransferase 11	1.71	0.007
Cyp4b1	NM_007823	Cytochrome P450, family 4, subfamily b, polypeptide 1	1.90	0.008
Acsl1	BI413218	Acyl-CoA synthetase long-chain family member 1	2.10	0.007
Hsd3b3	M77015	Hydroxy-delta-5-steroid dehydrogenase, 3 beta- and steroid delta-isomerase 3	2.24	0.002
Acox2	NM_053115	Acyl-Coenzyme A oxidase 2, branched chain	2.48	0.007
Ppara	BC016892	Peroxisome proliferator-activated receptor alpha	2.83	0.002
Angptl4	NM_020581	Angiopoietin-like 4	3.09	0.006
Mosc1	AA958845	MOCO sulfurase C-terminal domain containing 1	5.09	0.001
Proliferation				
Brdt	BG075871	Bromodomain, testis-specific	−1.74	0.005
Dtx3l	AV327407	Deltex 3-like	−1.68	0.010
Foxm1	BB398835	Forkhead box M1	1.71	0.005
Miscellaneous				
LOC622757	BC006659	Similar to transcription elongation factor B (SIII), polypeptide 2	−3.96	0.001
Zfp760	BB088782	Zinc finger protein 760	−2.70	0.004
Upk1b	BB427704	Uroplakin 1B	−2.09	0.002
ORF9	AF360358	Open reading frame 9 (PANDER)	−1.89	0.007
Zbtb8os	BB417508	Zinc finger and BTB domain containing 8 opposite strand	−1.73	0.007
Ankrd56	BB131927	Ankyrin repeat domain 56	−1.71	0.005

Table 4 (continued)

Gene symbol	Accession number	Gene name	Fold-change	*p*
Fbxo39	BB645745	F-box protein 39	−1.66	0.007
Cln8	AF125307	Ceroid-lipofuscinosis, neuronal 8	−1.51	0.002
Tmem20	BM121082	Transmembrane protein 20	1.54	0.010
Tmem64	BG075363	Transmembrane protein 64	1.59	0.007

The transcripts are considered to be modified when they have a fold-change ≥ 1.5 and $p \leq 0.01$. Reeler and control mice are compared. Three reeler and three control mice were used

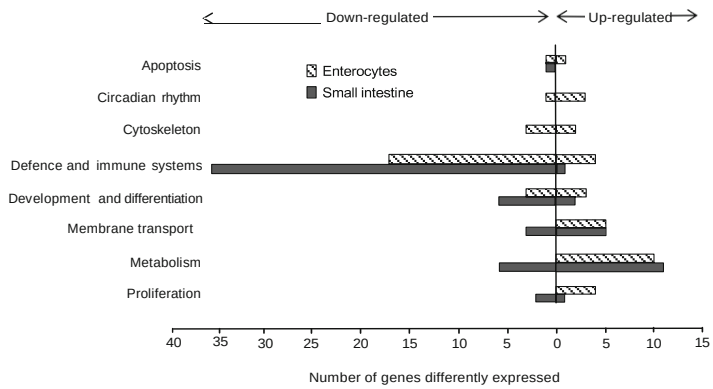

Fig. 2 Functional classifica- tion of the genes differentially modified by the reeler mutation. The differentially expressed genes obtained with the isolated epithelial cells samples microarray assay are represented separately from those obtained from the intact small intestine microarray assays

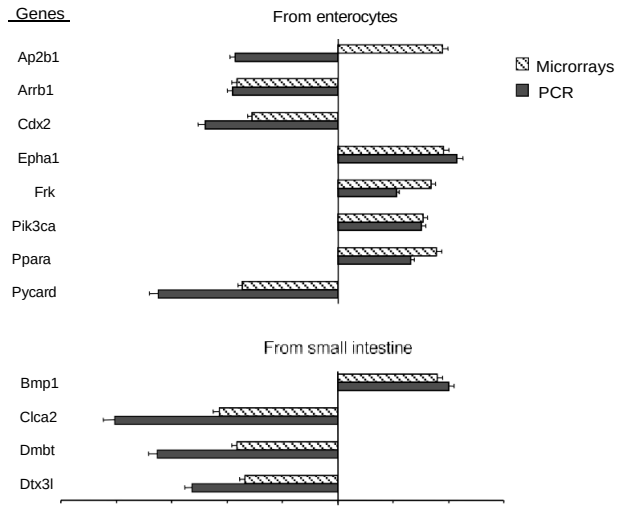

Fig. 3 Validation of the microarray results by real-time PCR analysis. Total RNA was obtained from either isolated epithelial cells or intact small intestine. The arbitrary units of relative mRNA abundance are compared with the fold-change values obtained in the microarray assay.
The data are the means ± SEM of three independent measurements. Three reeler and three control mice were used